

Fracture zone detection using very low frequency (VLF) electromagnetic method in parts of Oban Massif, southeastern Nigeria

George A. Michael¹, Abong A. Agwul² and Obi D. Akam³

¹*Department of Physics, University of Calabar, Calabar, Nigeria*

²*Department of Physics, Cross River University of Technology, Calabar, Nigeria*

³*Department of Geology, University of Calabar, Calabar, Nigeria*

ABSTRACT

Very low frequency (VLF) electromagnetic method was conducted to study fracture zone detection in parts of Oban Massif, Southeastern Nigeria. A total of twelve (12) profiles were covered during VLF data collection with 5m sample interval along each profile with spread length of between 120 and 650m. The VLF data were collected using ABEM Wadi instrument. The data were interpreted using KHFFILT software. The results of the study showed the presence of fracture zones and are prominently oriented in the NE-SW and NW-SE direction. The results also showed that most of the fracture zones were located at a depth range of 0 to 60m within the subsurface. The presence of and interconnectivity of the fracture zones show that the study area has good prospects for groundwater. The study therefore recommends the drilling of productive and sustainable boreholes at locations VLF 01, VLF 03, VLF 06, VLF 08, VLF 10 and VLF 12 between 125-175m, 230-300m, 50-150m, 200-290m, 275-400m and 200-225m respectively along the profile.

Key words: Fracture zone, very low frequency, Oban Massif, ABEM Wadi, groundwater

INTRODUCTION

The mapping of fracture zone which is a break in crystalline basement rock due to tectonic forces or intrusion of magmatic bodies is important for civil engineering and hydrogeological applications. In civil engineering, it helps to locate the safest depth to lay the foundation of buildings. The geological significance of fracture zones in hydrogeology is that it determines the competency of the underlie rocks. Areas that are extensively fractured and where the fractures are deep are considered as weak zones and considered suitable zones for groundwater development [12]. But areas that are slightly fractured and where fractures are not deep are considered as competent zones and are considered better sites for engineering purposes [13].

The drilling of test wells for fluid studies and the determination of hydraulic properties of subsurface rocks is an expensive method. Surface geophysical methods had been proven to be a rapid, inexpensive complement to drilling for determining the locations and orientation of fracture zone in bedrock [7]. They can be used in conjunction with geologic, hydrogeologic and borehole techniques to optimize well sitting [2] or as a 'stand alone' method of fracture detection [3], [4], [1] and assessment of leach ate plume migration in disposal sites [21].

In hard rock areas, groundwater is found in the cracks and fractures of the local rock. Groundwater yield depends on the size of fractures and their interconnectivity. VLF EM method has been applied successfully to map the resistivity contrast at boundaries of fractured zones having a high degree of connectivity [9]. Also VLF method yields a higher depth of penetration in hard rock areas because of their high resistivity [11]. VLF method is capable of delineating fractures in lateral direction effectively compared to resistivity sounding [10], characterize aquifer structures in a

complex environment [18], underground water contamination by solid waste [19], examine the fault pattern of industrial estate [20].

This study was driven by the desire to investigate water bearing fracture zones in parts of Oban Massif using very low frequency (VLF) electromagnetic method. Most boreholes drilled in the past in the area are unproductive and due to this failure, it is therefore necessary to use an appropriate geophysical method to locate the fracture zones. This became important as the inhabitants in the study area depend solely on streams, lakes and groundwater for their domestic needs.

Location

The study area comprises eight (8) villages namely, Awi, Ayaebam, Mbarakom, Akamkpa, Okom Ita, Igbofia, Uyanga and Ojorin Akamkpa Local Government Area of Cross River State. These villages are within the Oban Massif basement complex which is situated between latitudes 5°15'N-5°30'N and longitudes 8°10'E-8°25'E in the south eastern part of Nigeria extending into the neighboring Cameroon (Fig 1.0). The villages are accessible through untarred roads which are offset of Calabar-Ikom highway. There are residential buildings, markets, toilet near the villages.

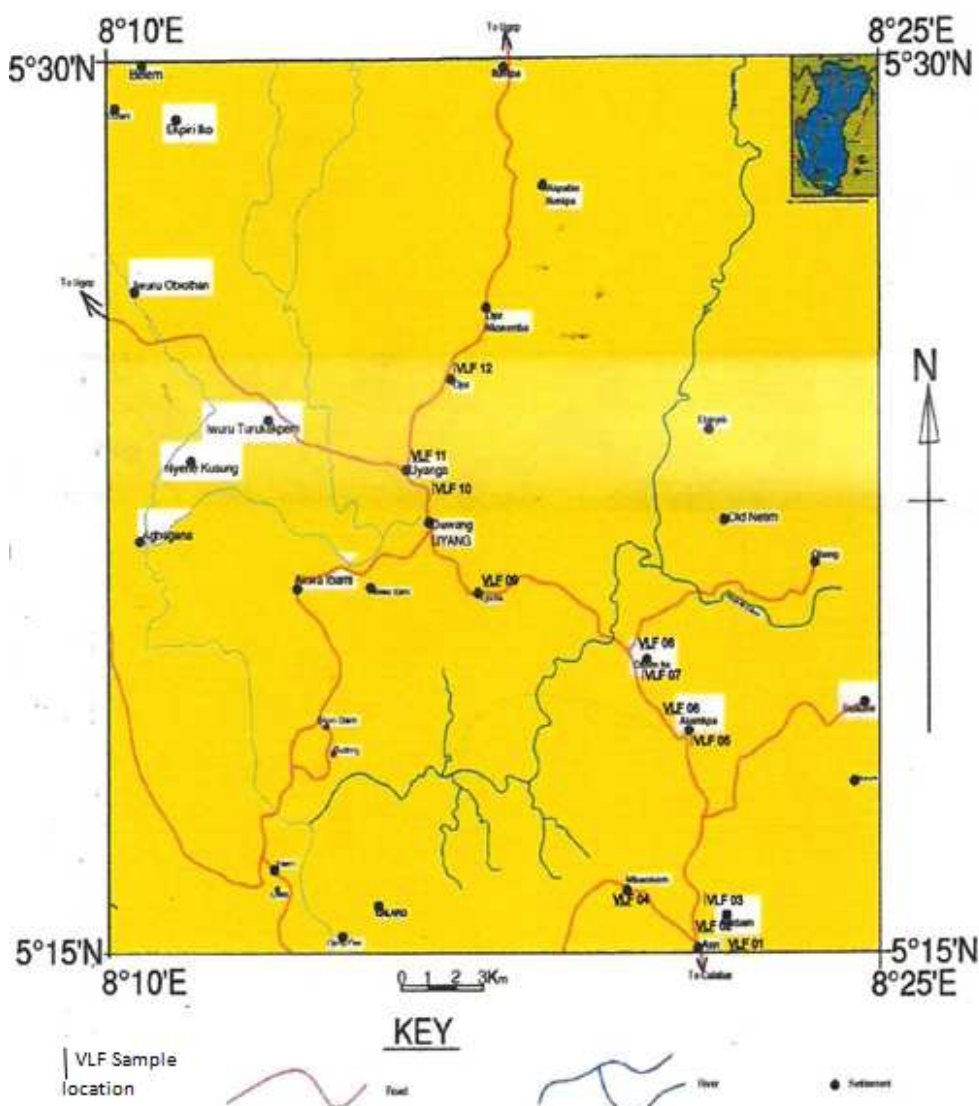


Fig 1: Location map showing the study area (Drawing Unit, Dept. of Geology, UNICAL, 2012)

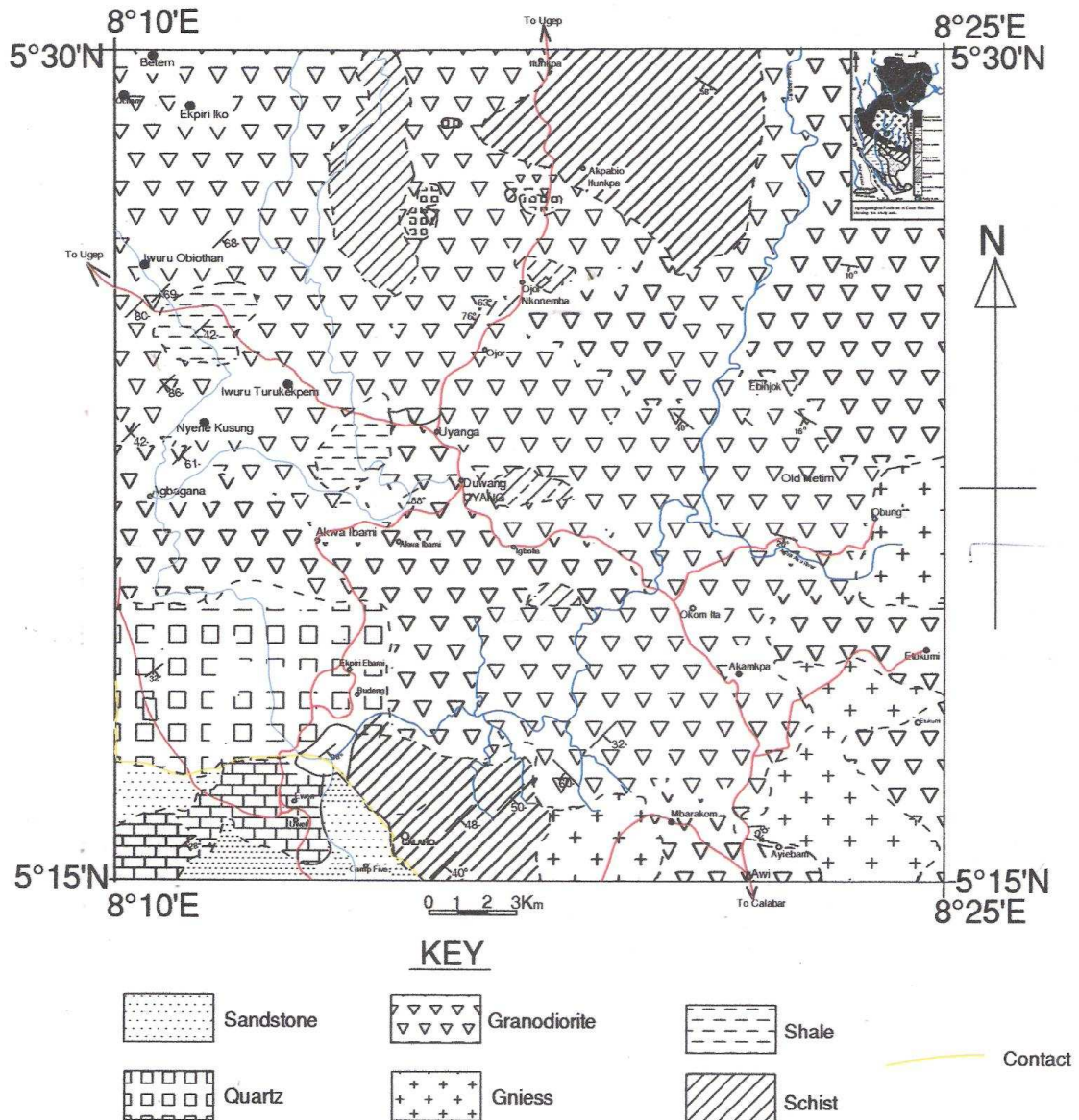


Fig 2: Geologic map of the study area (Oban Massif). (Drawing Unit, Dept. of Geology, UNICAL, 2012)

Hydrogeology and Geology of the study area

The study area belongs to the climatic region of Nigeria called the subequatorial South [8]. It shows the characteristic features of the humid tropics, that is high temperature, high rainfall and high humidity. The seasonal conditions of the area are wet and dry seasons. The wet season spans a period of about six months (May to October) and the dry season lasts from (November to April) [8]. These wet and dry seasons bring about expansion and contraction of rocks which ultimately trigger-off weathering process in the area. The total annual rainfall is between 150cm-200cm and the highest temperatures are recorded in the day and lowest in the night at all seasons [8]. These temperatures and rainfall fluctuation greatly accelerate weathering and also induce thick vegetation cover. Prominent relief features include hills, valleys, ridges, rivers, stream channels. The drainage pattern is dendritic. Movement of streams is controlled by joints and fractures.

The Oban Massif is made up of two main sectors namely, the western sector (topographically sub-dued with higher human population density) and the eastern sector (topographically rugged country with peaks forested up to summits and sparse human settlements [17]. The western sector is made up of gneisses, granites, quartzite, schist, dolerites, granodiorites and pegmatite [14], while the east is composed of migmatites, biotite-hornblende-gneisses, granites and amphibolites [15]. The Oban massif is underlain by highly deformed Precambrian crystalline rocks, mainly

granites, gneisses and schist. These rocks exhibit varying degrees of weathering across the massif. They are intruded by pegmatite, granodiorites, diorites, tonolites, monzonites, charnokites and dolerites [5] and [6].

The area has a complex terrain and the differentiation of the rock types had remained difficult. One of this difficulty stems from the location of the Oban Massif which is in the thick equatorial rain forest highly populated by wildlife. Secondly, rock outcrops in the area are generally intensely weathered and this makes it difficult to obtain fresh rock for geologic studies. The oldest rock in the Oban Massif is the banded gneisses and dolerite is the youngest.

Economic minerals that abound within the basement complex comprise feldspars, galena, gemstones, graphite, gold, ilmenite, kaolin, manganese, mica, quartz, rutile, tin and uranium [16].

MATERIALS AND METHODS

The survey was carried out using ABEM Wadi VLF instrument with other accessories such as hand-held Global Positioning System (GPS) and measuring tape. A total of twelve (12) VLF EM profile stations were conducted in the eight (8) villages with profile length ranging from 120 to 650m. Readings were taken at station interval of 5m in the twelve locations with profile lines oriented in N-S, E-W directions respectively. The data were collected along a traverse and the traverse was perpendicular to the strike. During survey, effort was made to avoid putting traverses in area that contain cultural features that may mask anomalies associated with the intended target strike. Also the direction of the transmitting station was perpendicular or nearly perpendicular to the traverse before readings were taken. The profiles were denoted as VLF 01 to VLF 12.

RESULTS AND DISCUSSION

The KHFFILT software was used in the interpretation of the data along VLF traverses which shows both positive Fraser and Karous-Hjelt anomalies and negative Fraser and Karous-Hjelt anomalies along the traverses and indication of the probable fracture zones along each of the traverses. For each sample point, a plot of the raw field data, the Fraser filtered data and the Karous-Hjelt plots are displayed (Fig 3-Fig 38).

At location VLF 01 with traverse oriented in the E-W direction, a plot of filtered data shows prominent positive response between 125-175m (Fig 4) resulting in probable fracture zone located between 125-175m along the profile at a depth extending from 0-60m oriented at NW-SE direction (Fig 5).

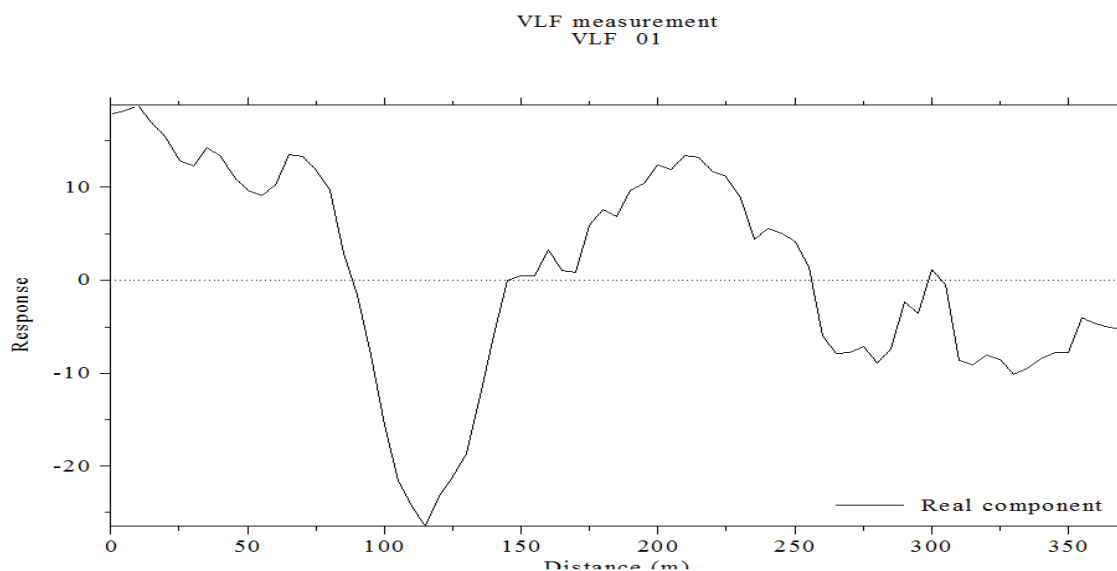


Fig 3: A plot of unfiltered in-phase data against distance at location VLF 01

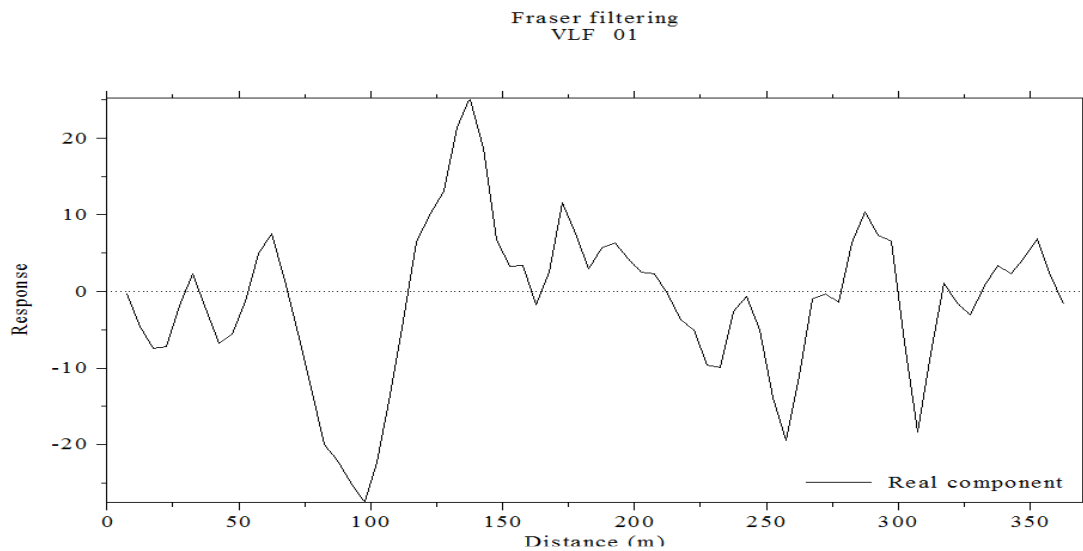


Fig 4: A plot of filtered in-phase data against distance at location VLF 01

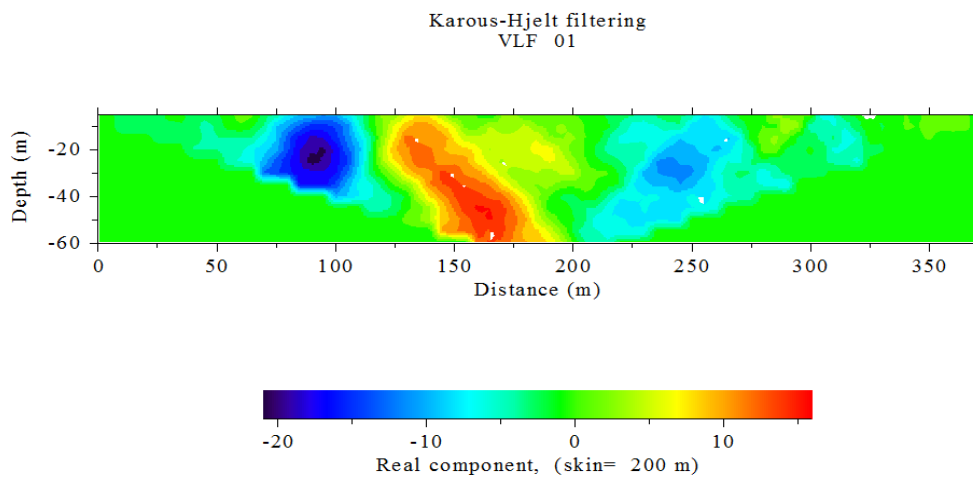


Fig 5: Current density cross section plot of in-phase data against distance at location VLF 01

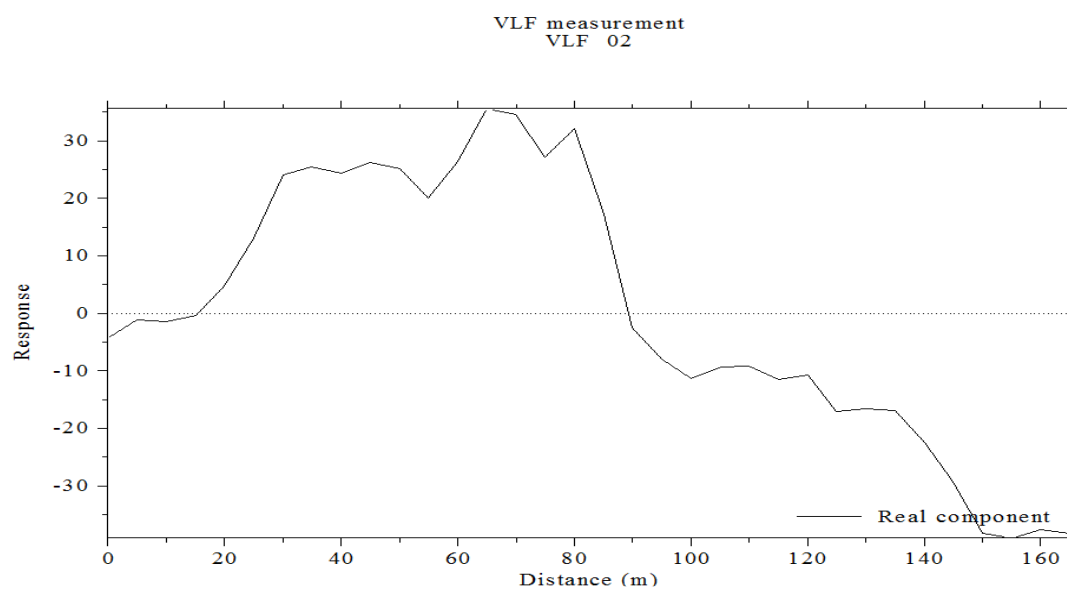


Fig 6: A plot of unfiltered in-phase data against distance at location VLF 02

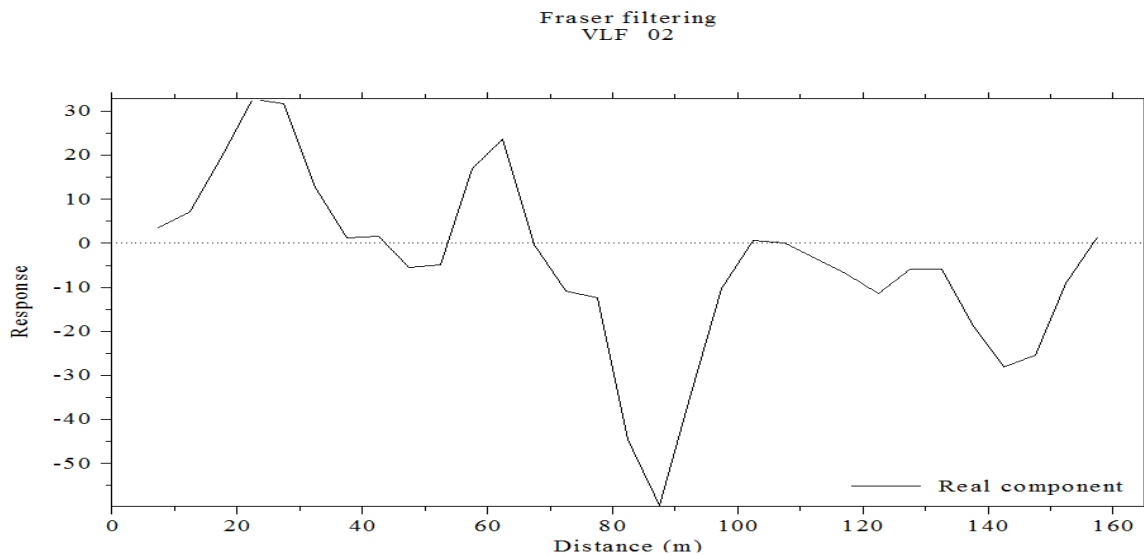


Fig 7: A plot of filtered in-phase data against distance at location VLF 02

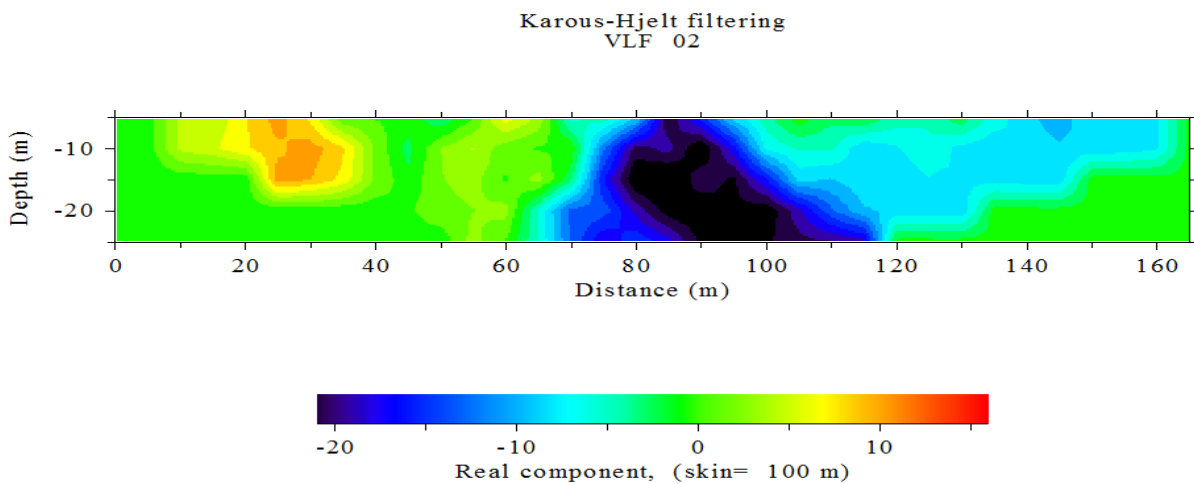


Fig 8: Current density cross section plot of in-phase data against distance at location VLF 02

At location VLF 02 with traverse oriented in the E-W direction, a not well-fractured zone with positive Fraser filter was identified (Fig 7). This zone is located at a horizontal distance of between 20-30m, along the profile at depth of between 0-20m. This zone is oriented at NW-SE (Fig 8).

At location VLF 03 with traverse oriented in the N-S direction, two (2) probable fracture zones were identified with one highly conductive. They were located between 50-70m and 230-300m respectively along the profile (Fig 10). The depth of each fracture zone was between 0-30m and 0-60m with orientation sat NE-SW and NW-SE respectively (Fig 11).

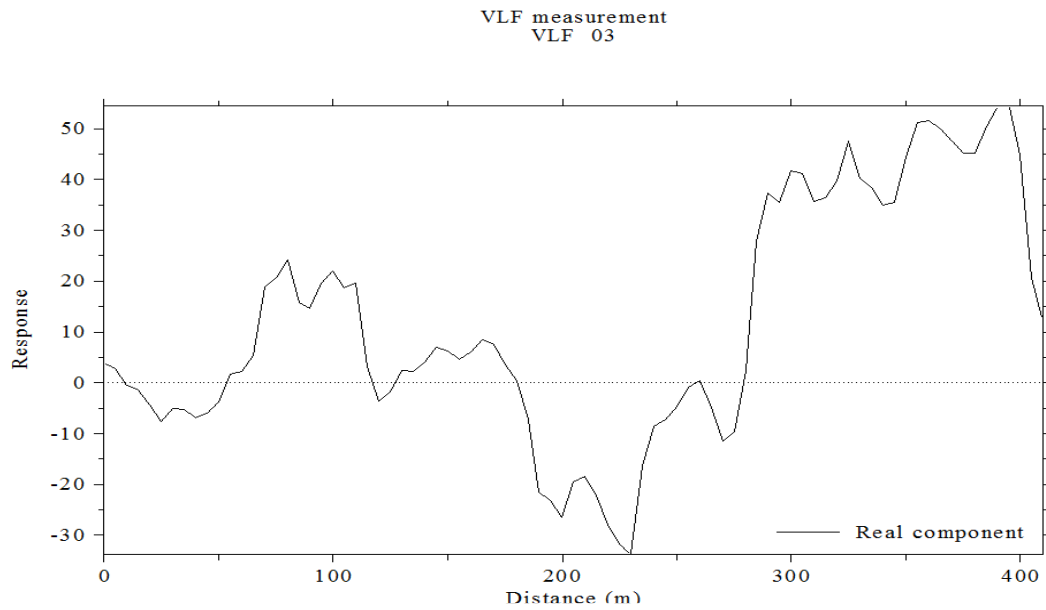


Fig 9: A plot of unfiltered in-phase data against distance at location VLF 03

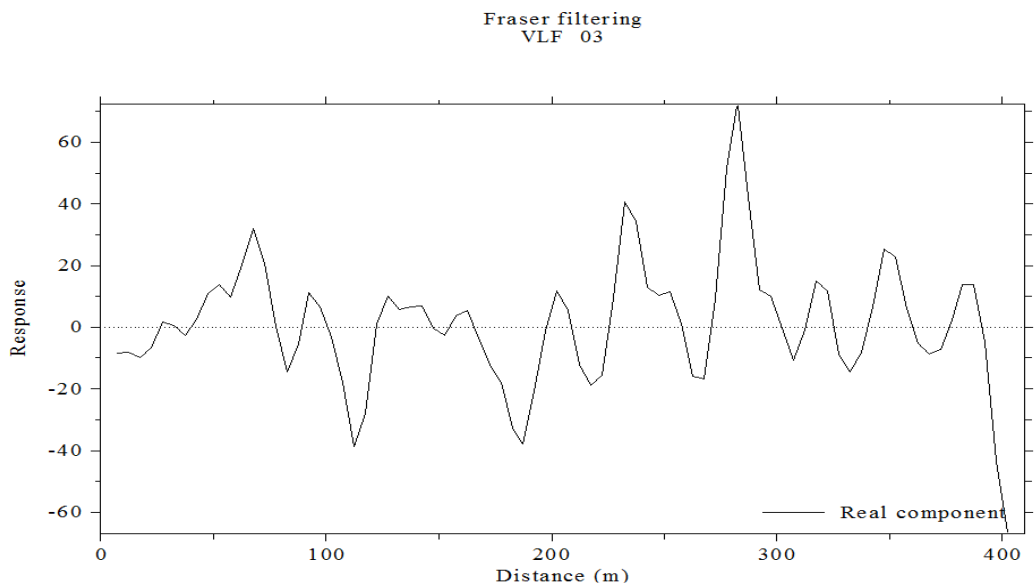


Fig 10: A plot of filtered in-phase data against distance at location VLF 03

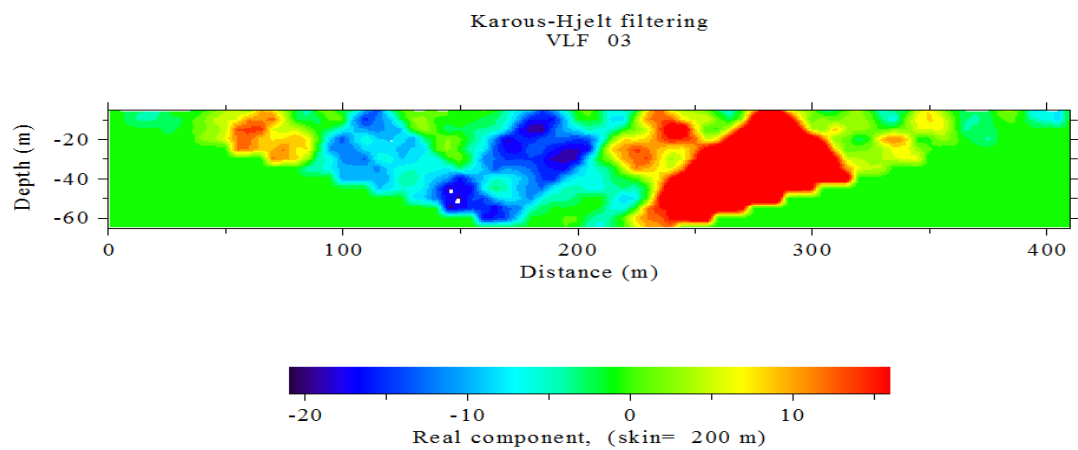


Fig 11: Current density cross section plot of in-phase data against distance at location VLF 03

At location VLF 04 with traverse oriented in the E-W direction (Fig 13), three (3) probable but not well-fractured zones were identified. They were located between 15-30m, 45-75m and 90-110m along the profile. The depth of each zone was between 0-15m, 0-20m and 0-15m all oriented at N-S respectively (Fig 14).

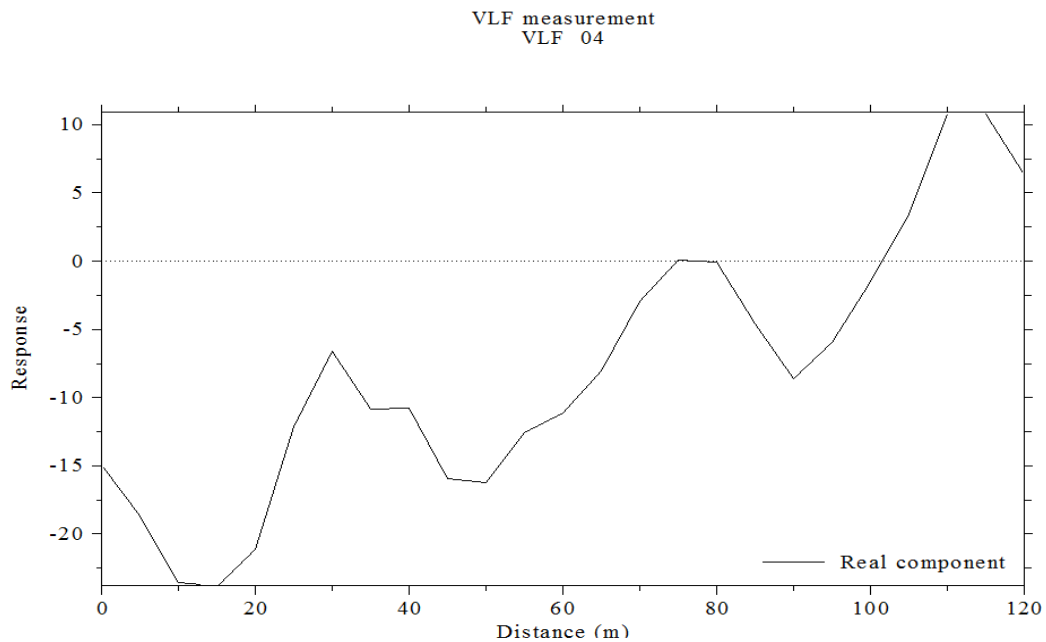


Fig 12: A plot of unfiltered in-phase data against distance at location VLF 04

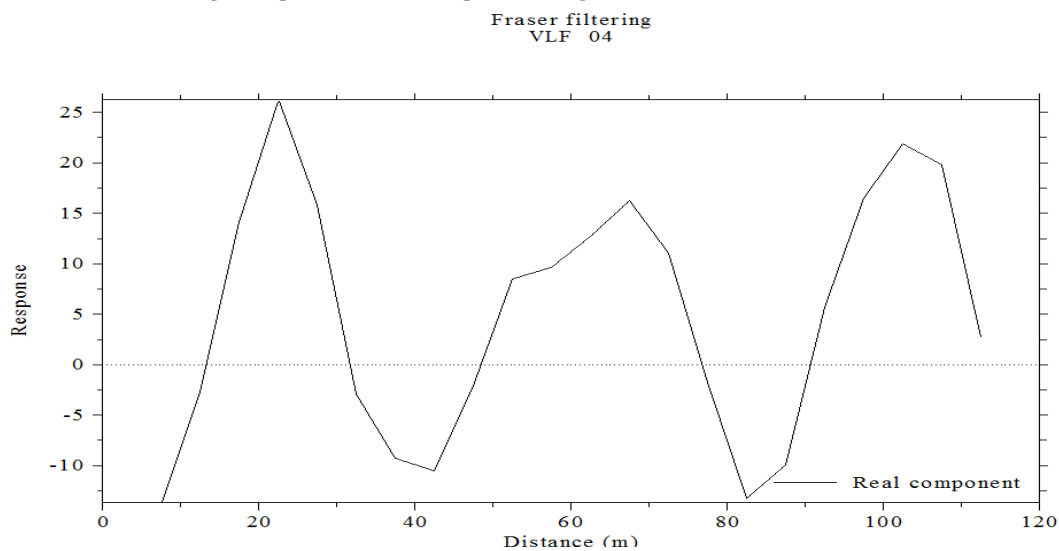


Fig 13: A plot of filtered in-phase data against distance at location VLF 04

The result of VLF data collected at location VLF 05 with traverse oriented in E-W direction (Fig 16) shows two (2) positive but not well-fractured Fraser filter responses along the horizontal distance between 90-100m and 350-370m with depth extending from 0-60m and 0-80m. They were oriented at NW-SE and NE-SW respectively (Fig 17).

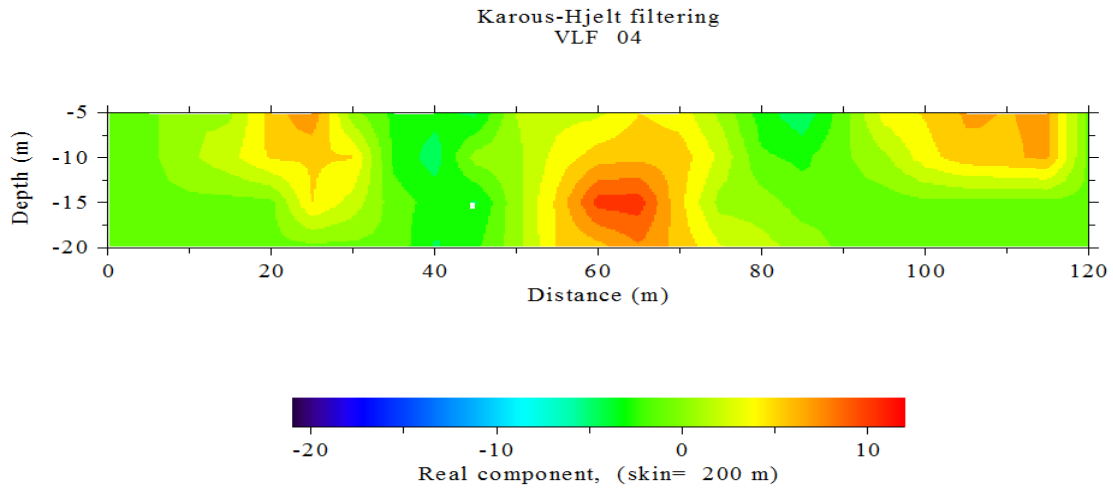


Fig 14: Current density cross section plot of in-phase data against distance at location VLF 04

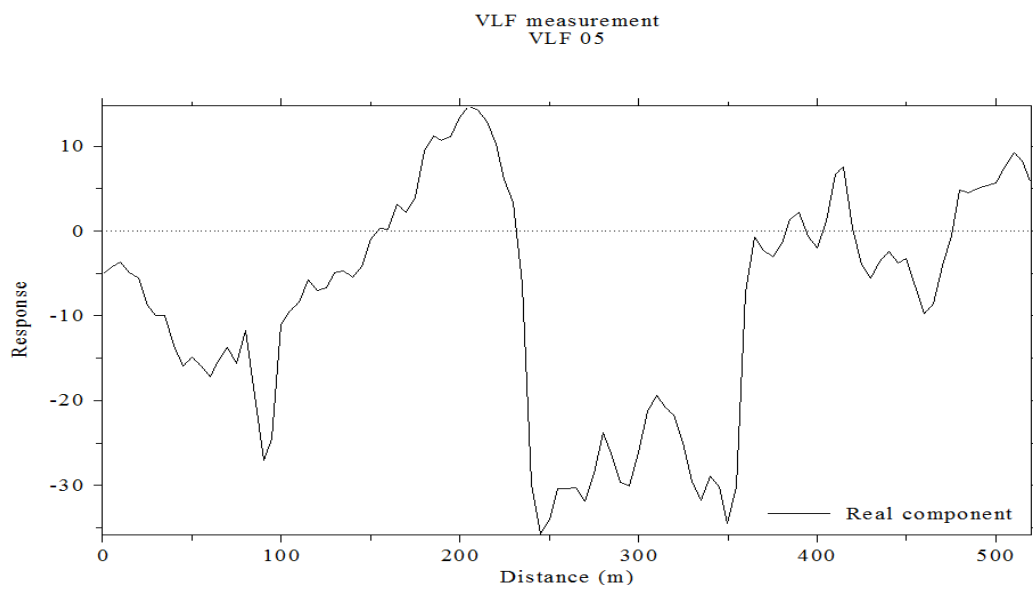


Fig 15: A plot of unfiltered in-phase data against distance at location VLF 05

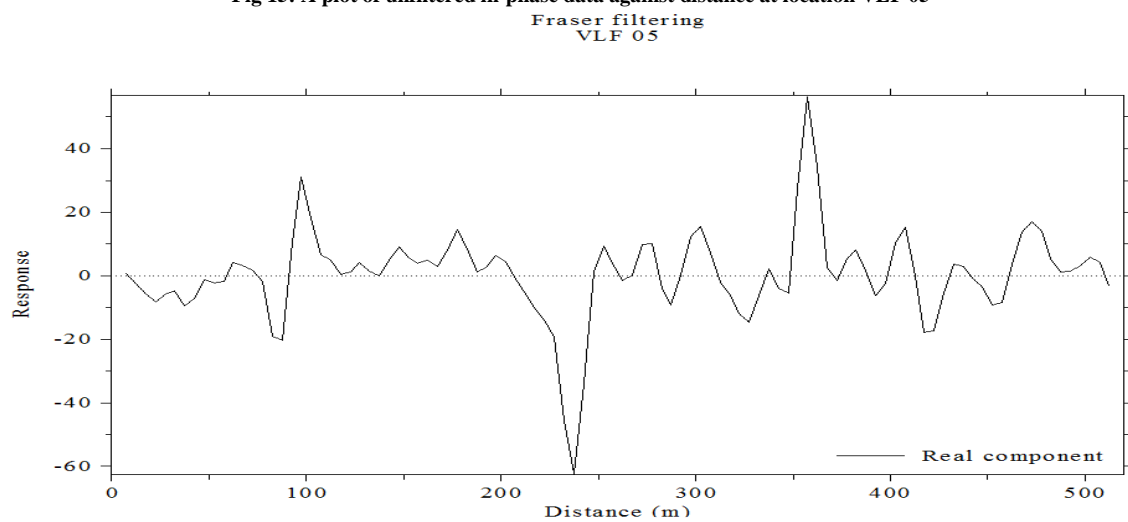


Fig 16: A plot of filtered in-phase data against distance at location VLF 05

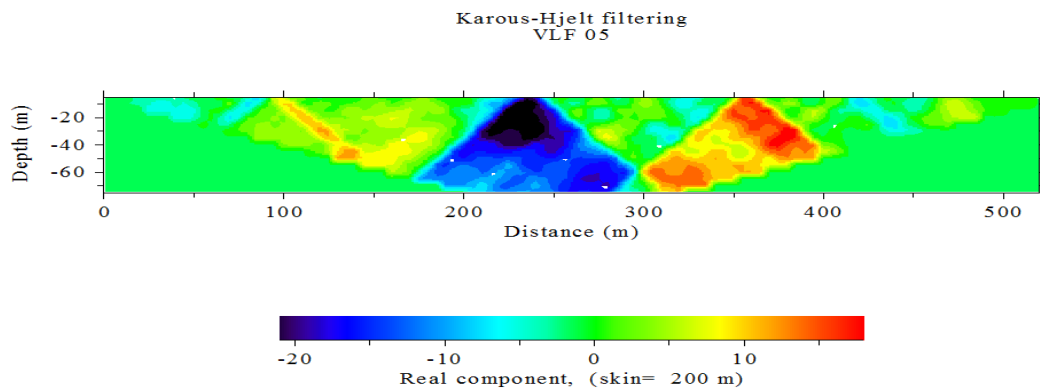


Fig 17: Current density cross section plot of in-phase data against distance at location VLF 05

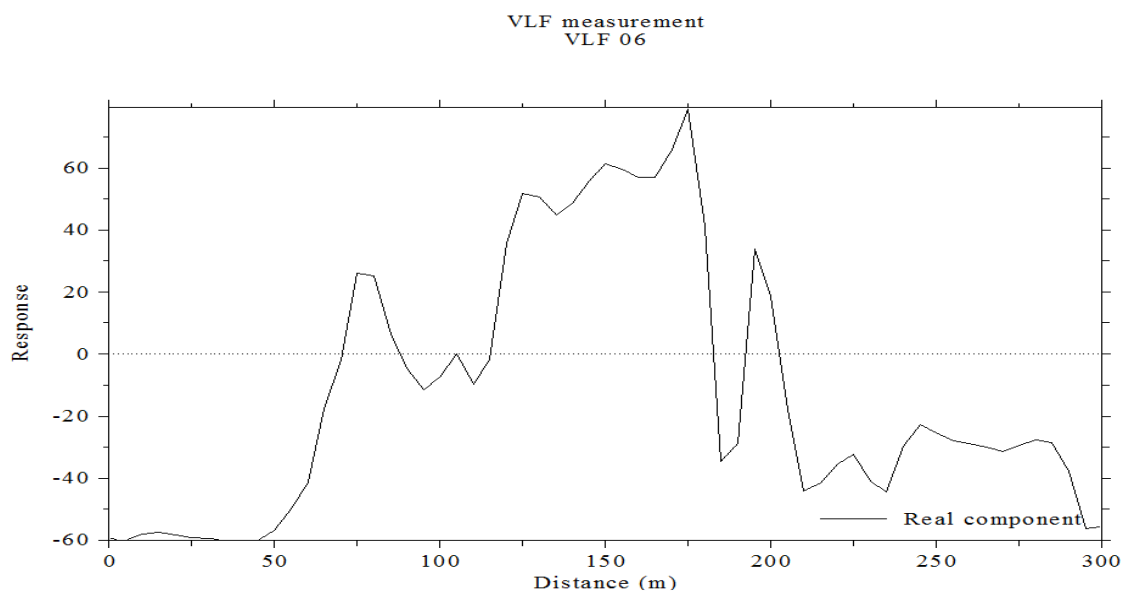


Fig 18: A plot of unfiltered in-phase data against distance at location VLF 06

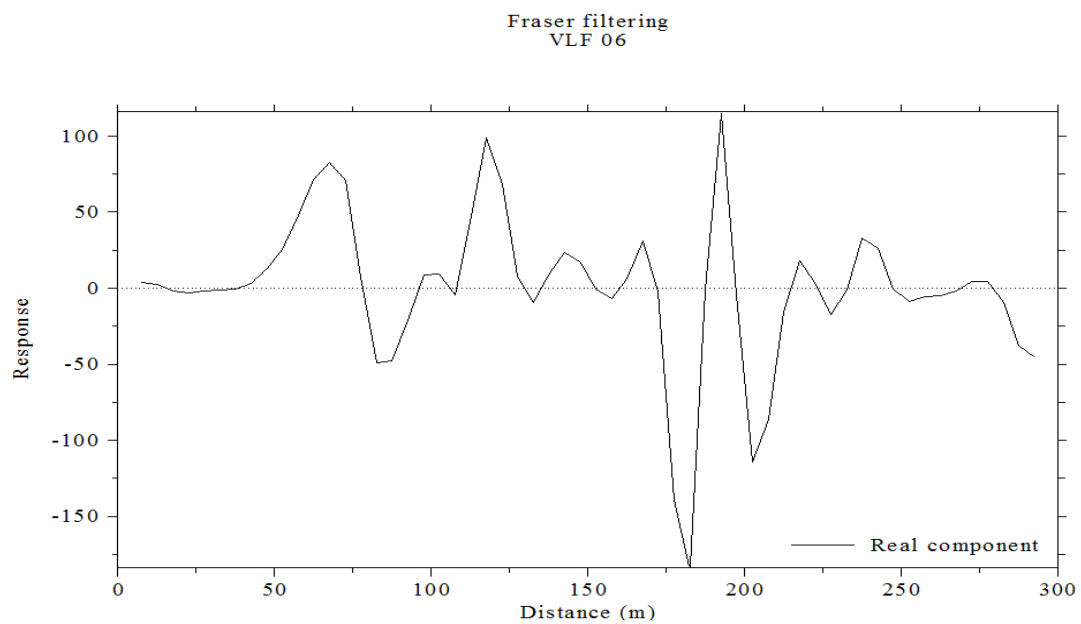


Fig 19: A plot of filtered in-phase data against distance at location VLF 06

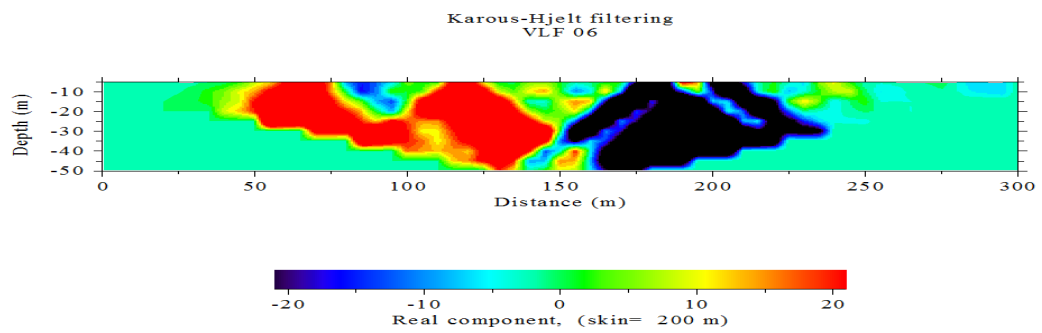


Fig 20: Current density cross section plot of in-phase data against distance at location VLF 06

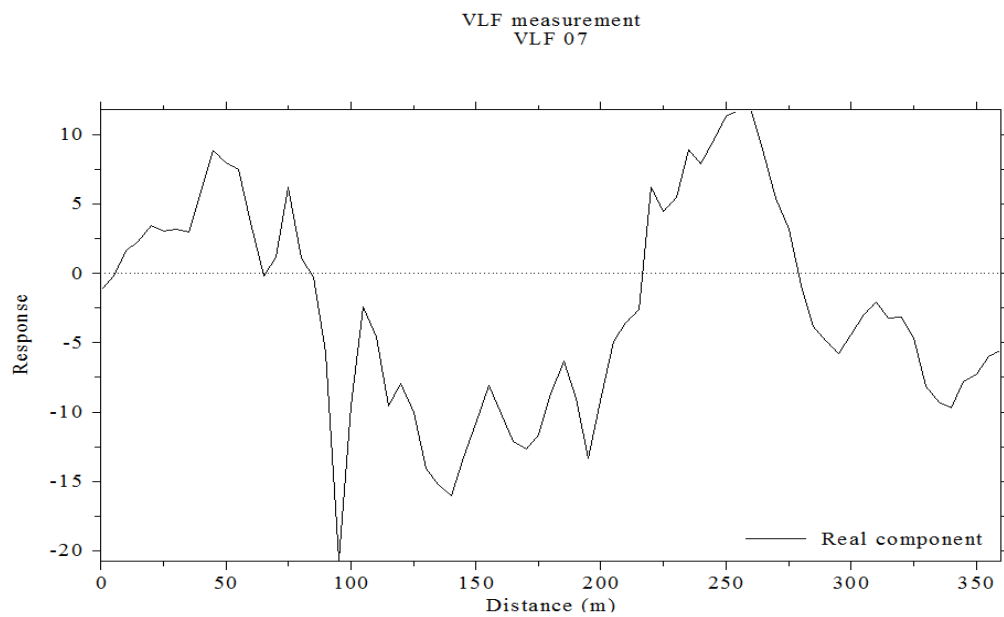
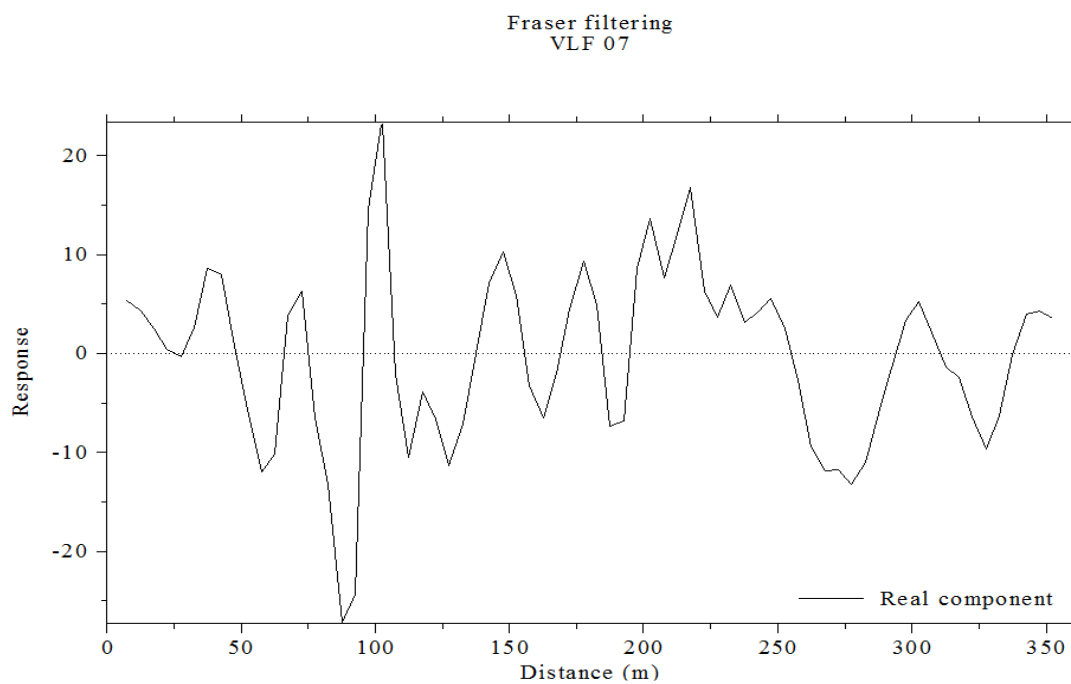


Fig 21: A plot of unfiltered in-phase data against distance at location VLF 07



22: A plot of filtered in-phase data against distance at location VLF 07

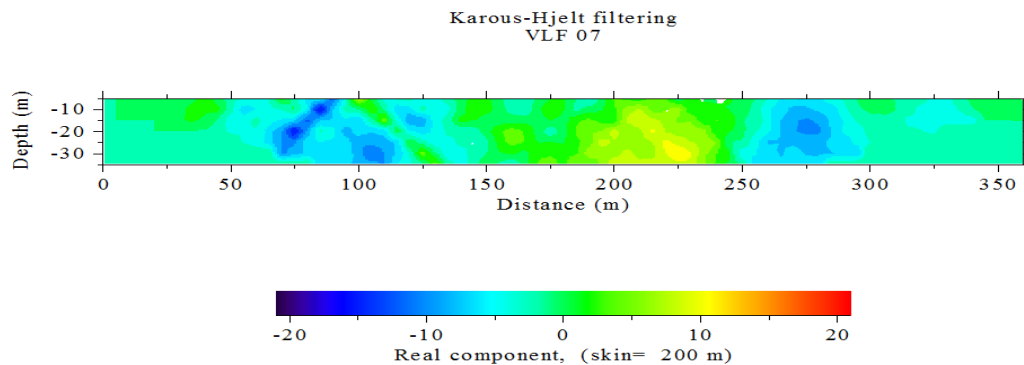


Fig 23: Current density cross section plot of in-phase data against distance at location VLF 07

The result of the VLF plot at location 06 with traverse oriented in the N-S direction shows positive responses along the profile between 50-150m (Fig 19) resulting in a probable fracture zones that are interconnected to each other at depth from 0-40m and 0-50m oriented at NE-SW (Fig 20).

The VLF responses at location VLF 07 with traverse oriented in the E-W direction shows positive responses along the traverse (Fig 22) resulting in a not pronounced fracture zones located between 180-240m (Fig 23).

At location VLF 08 with traverse oriented in the N-S direction, the plot of the filtered data shows positive responses closely connected zones along the traverse (Fig 25) between 75-175m and between 200-290m with depth extending from 0-60m and 0-65m oriented at NE-SW and NW-SE respectively (Fig 26).

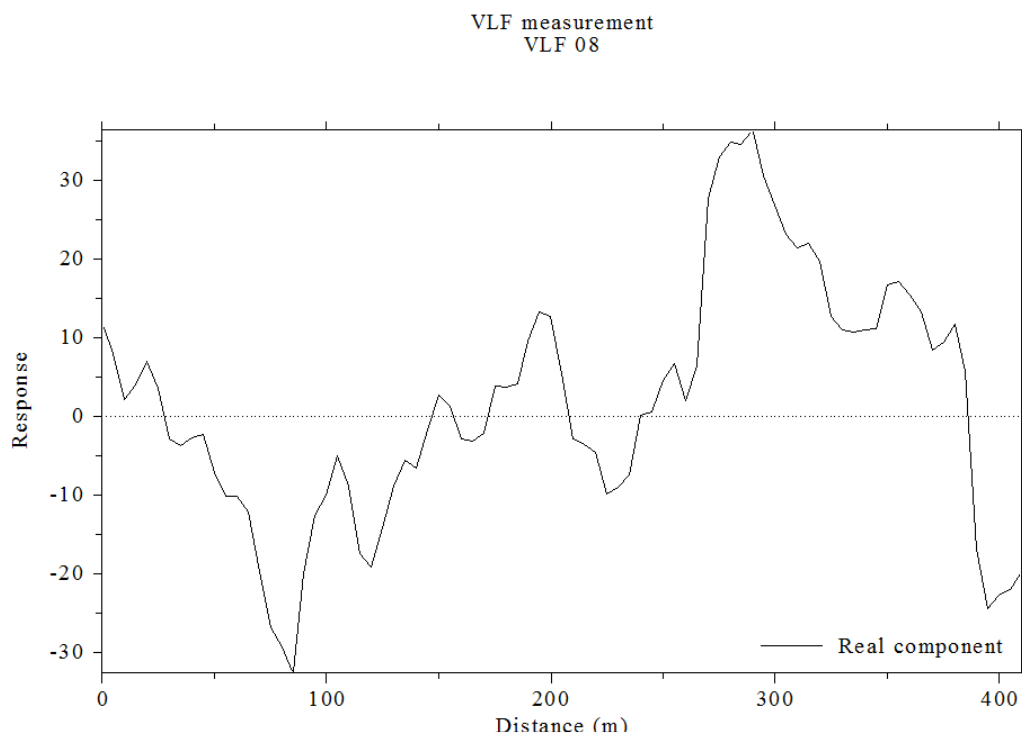


Fig 24: A plot of unfiltered in-phase data against distance at location VLF 08

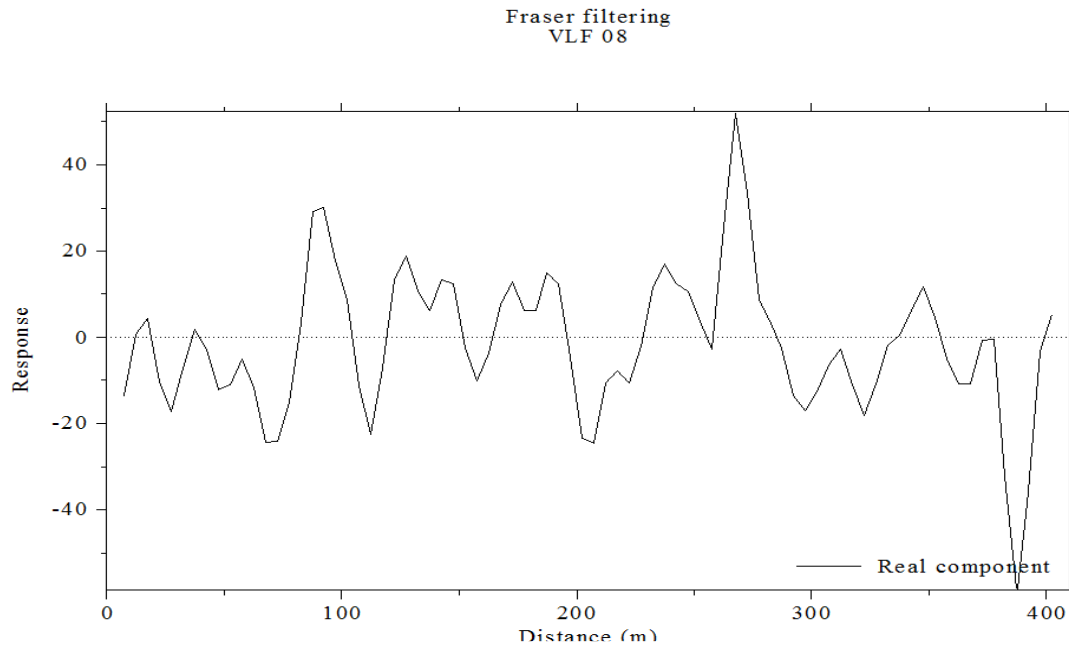


Fig 25: A plot of filtered in-phase data against distance at location VLF 08

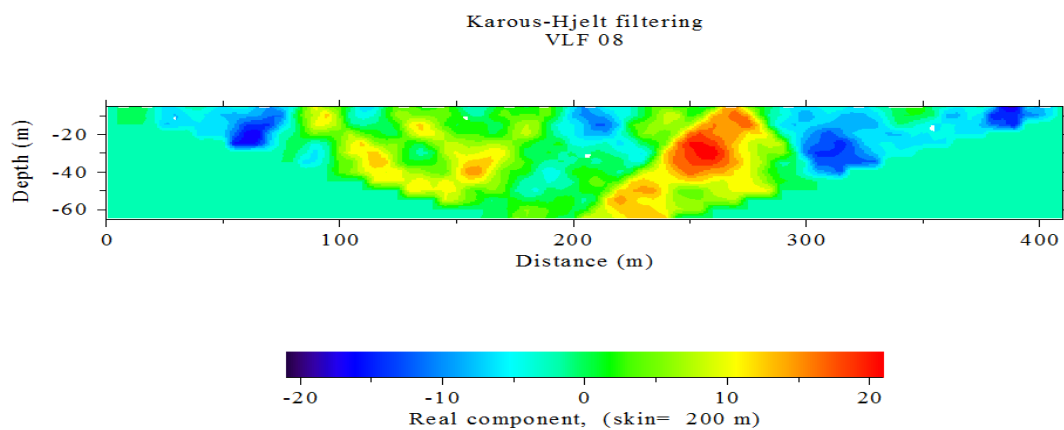


Fig 26: Current density cross section plot of in-phase data against distance at location VLF 08

At location VLF 09 with traverse oriented in the E-W direction, three (3) positive responses position were identified along the traverse (Fig 28), these were between 75-100m, 250-300m and 350-400m respectively. These correspond to weak zone located at depth between 0-40m, 0-80m and 0-60m (Fig 29).

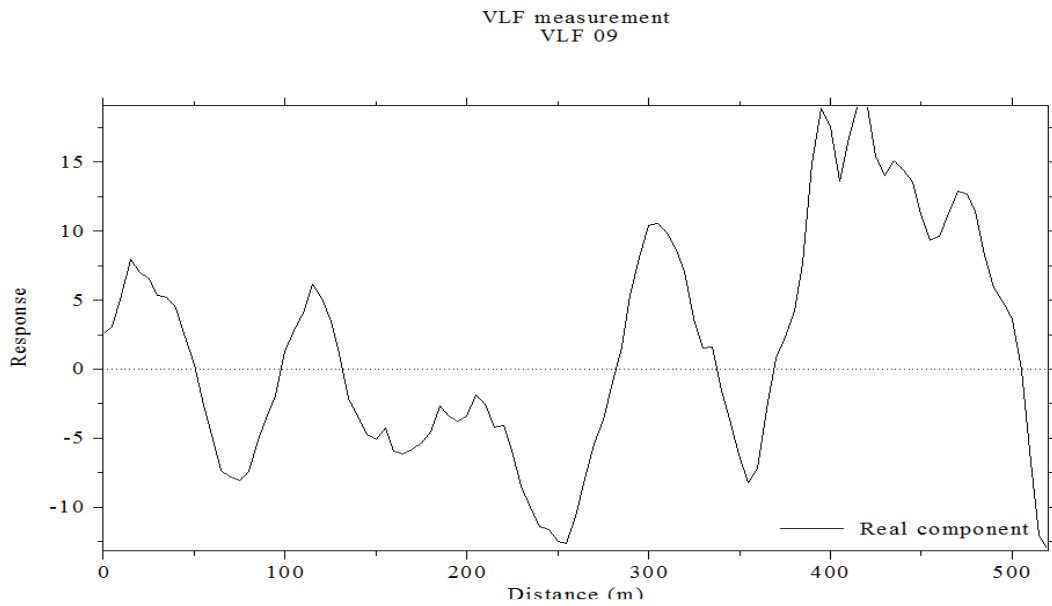


Fig 27: A plot of unfiltered in-phase data against distance at location VLF 09

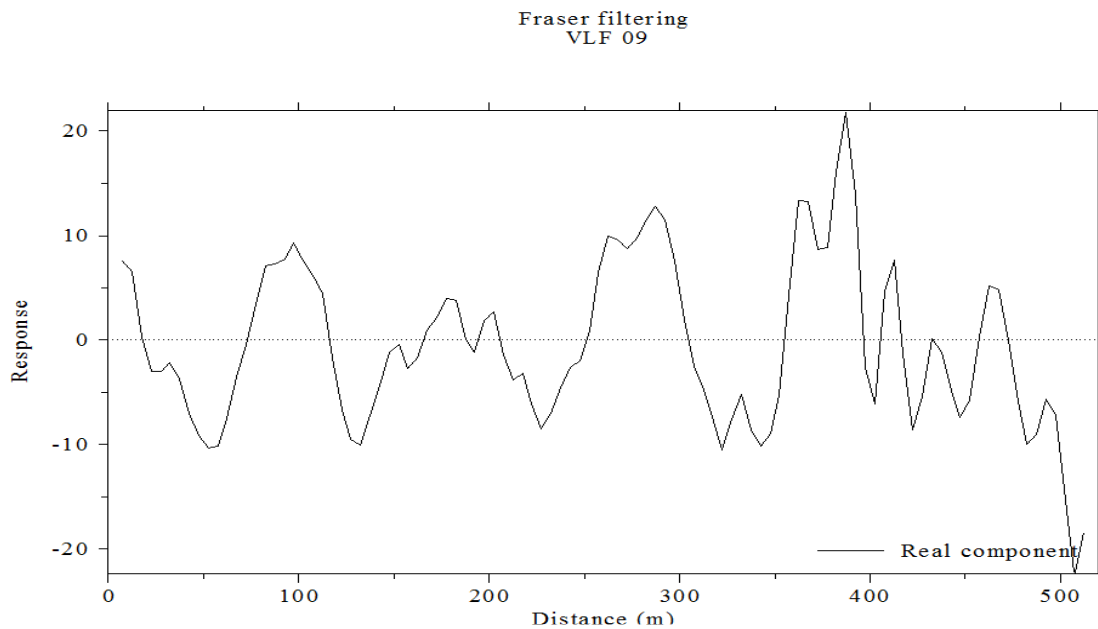


Fig 28: A plot of filtered in-phase data against distance at location VLF 09

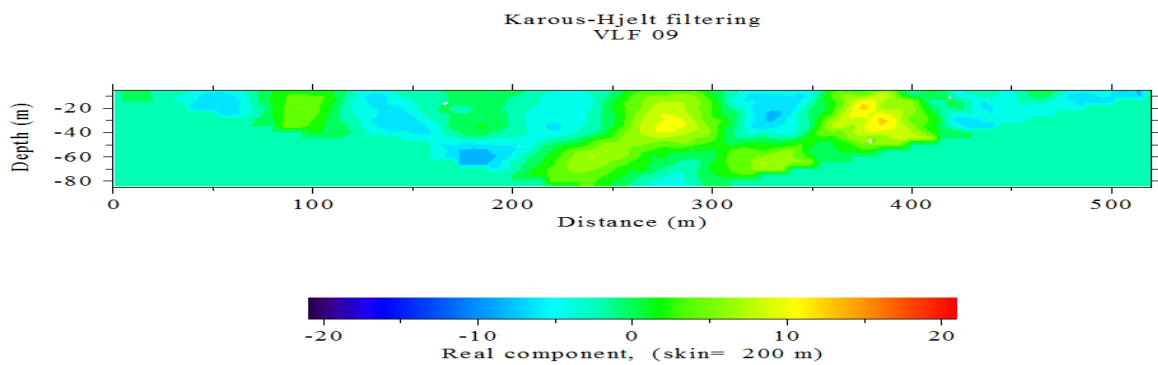


Fig 29: Current density cross section plot of in-phase data against distance at location VLF 09

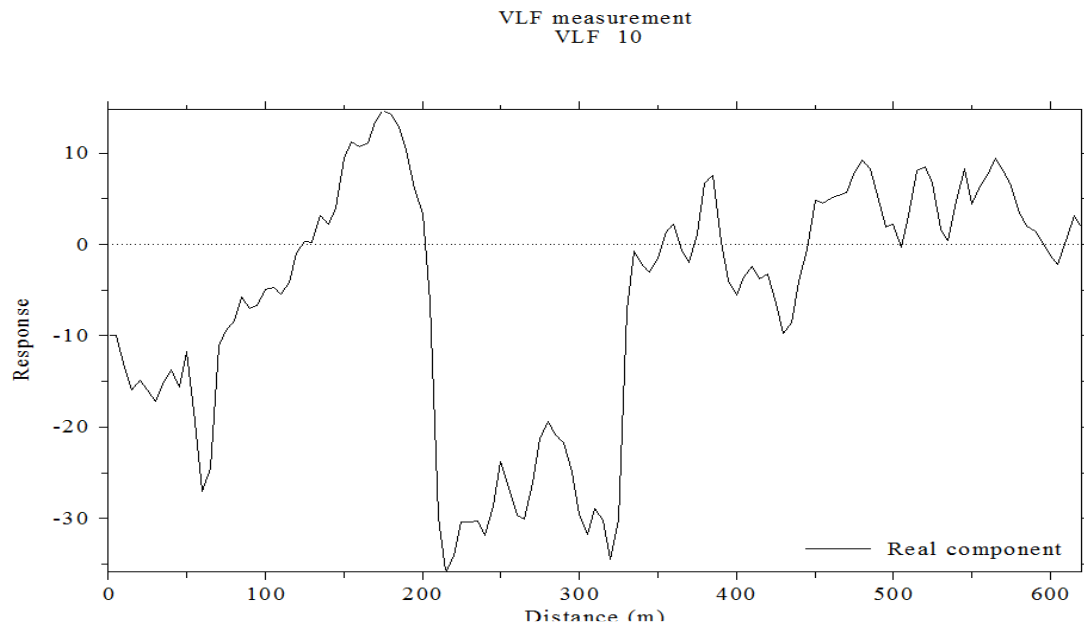


Fig 30: A plot of unfiltered in-phase data against distance at location VLF 10

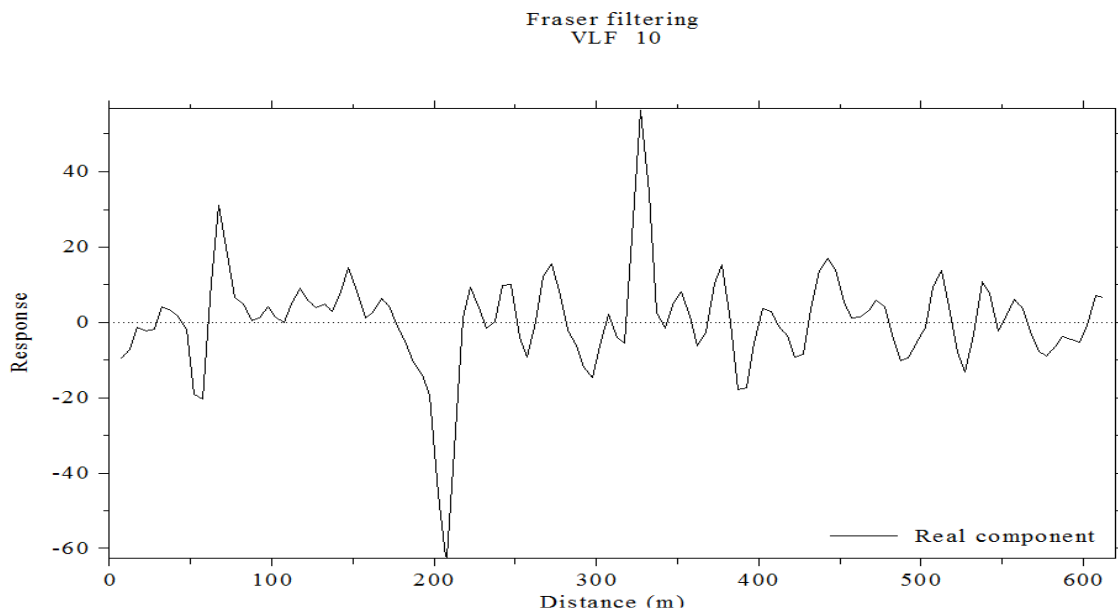


Fig 31: A plot of filtered in-phase data against distance at location VLF 10

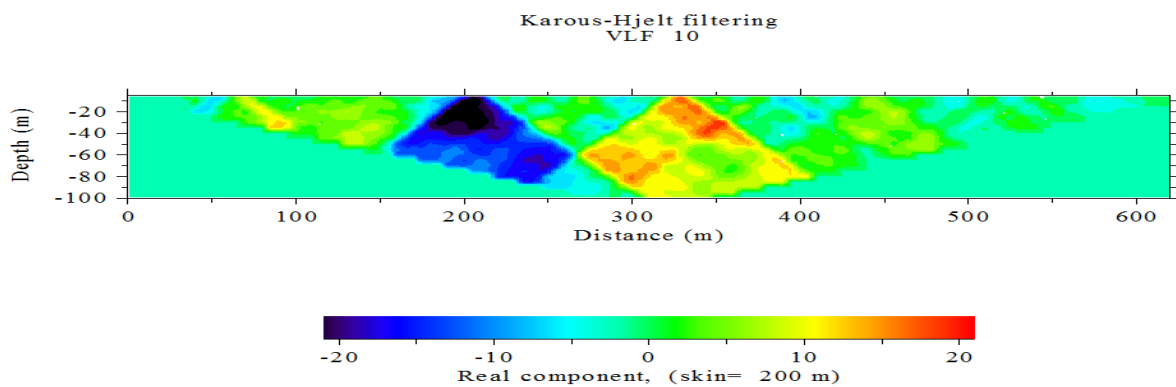


Fig 32: Current density cross section plot of in-phase data against distance at location VLF 10

The result of the plot at location VLF 10 with traverse oriented in the E-W direction shows positive responses between 50-150m, 275-400m along the traverse (Fig 31) resulting in a probable fracture zone and a weak zone along the traverse with depth extending from 0-60m, 0-100m oriented at NW-SE respectively (Fig 32).

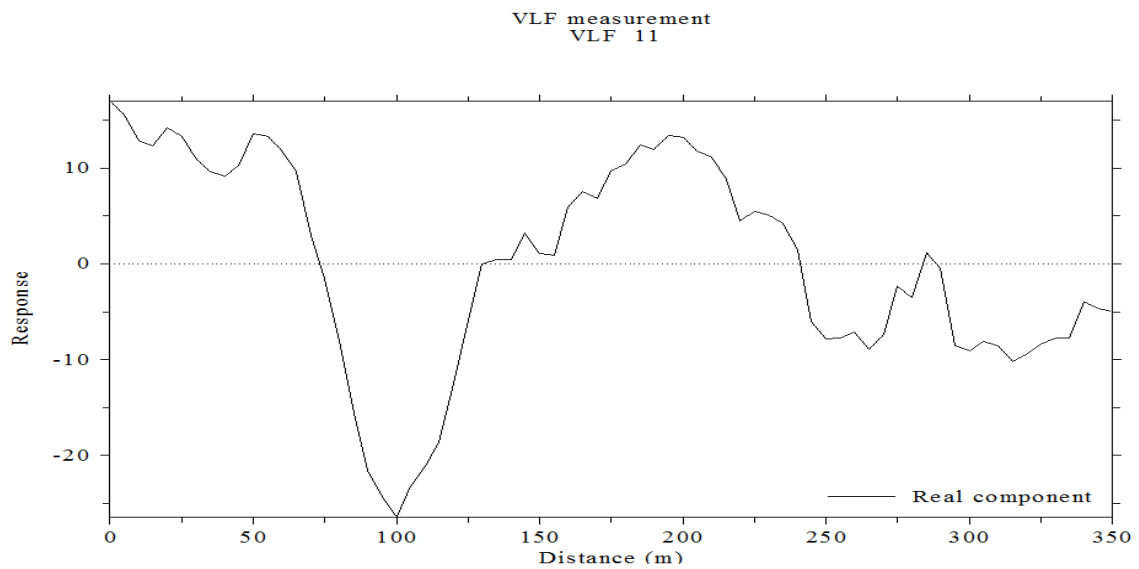


Fig 33: A plot of unfiltered in-phase data against distance at location VLF 11

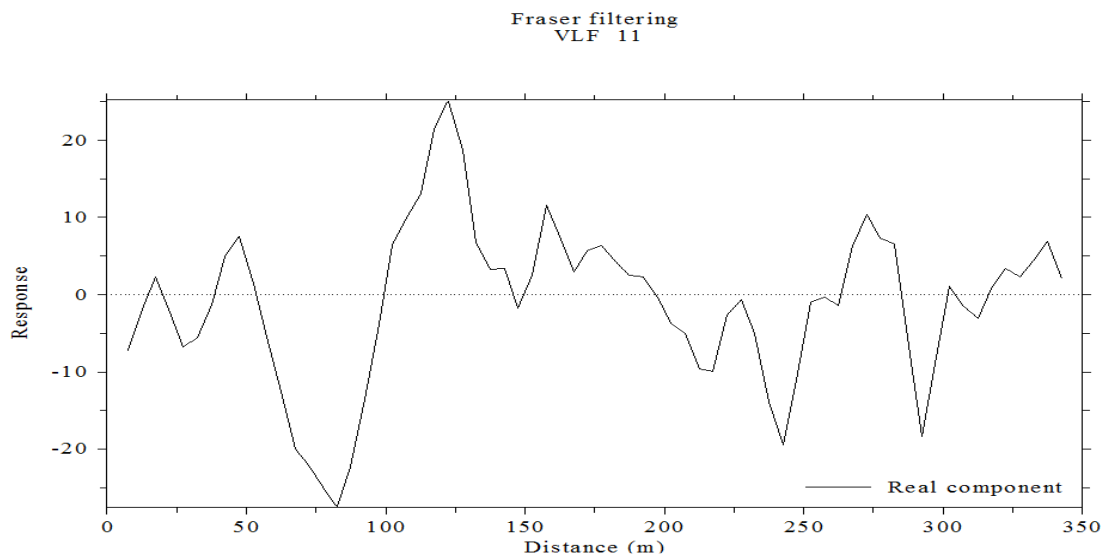


Fig 34: A plot of filtered in-phase data against distance at location VLF 11

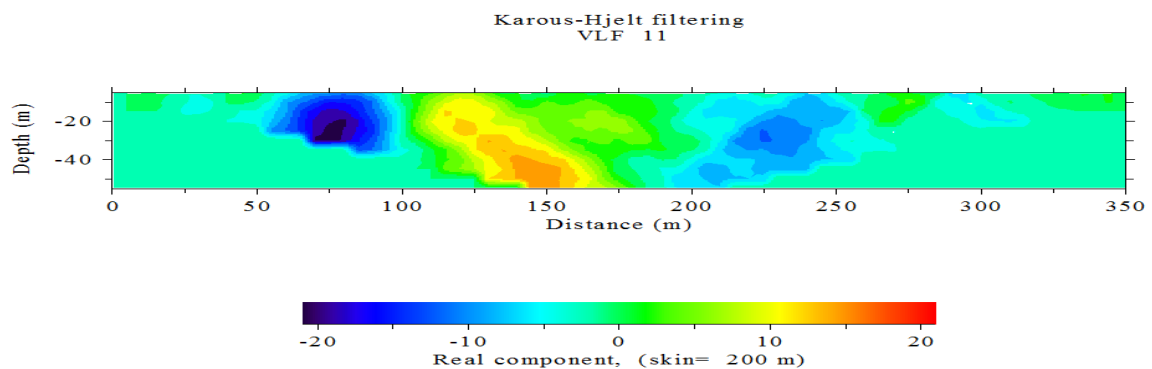


Fig 35: Current density cross section plot of in-phase data against distance at location VLF 11

At location VLF 11 with traverse in the N-S direction shows positive response between 100-175m along the traverse (Fig 34). The corresponding probable fracture is located at depth extending from 0-60m oriented at NE-SW (Fig 35).

At VLF 12 with traverse oriented in the N-S direction (Fig 37) one prominent positive Fraser filter response was identified. It is located between 200-225m at depth extending from 0-40m oriented at NW-SE (Fig 38).

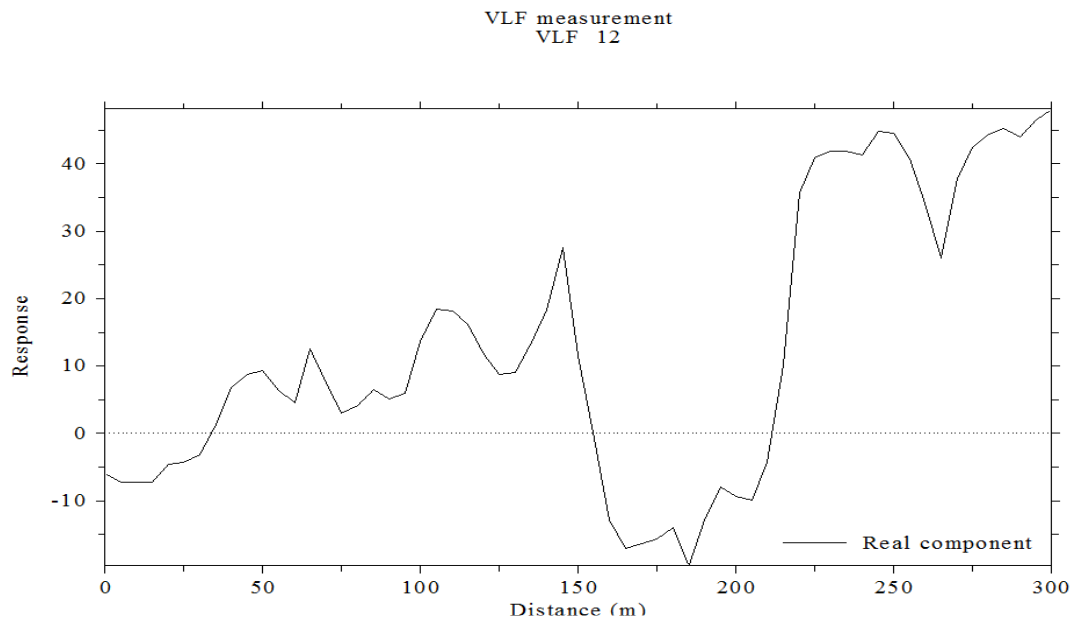


Fig 36: A plot of unfiltered in-phase data against distance at location VLF 12

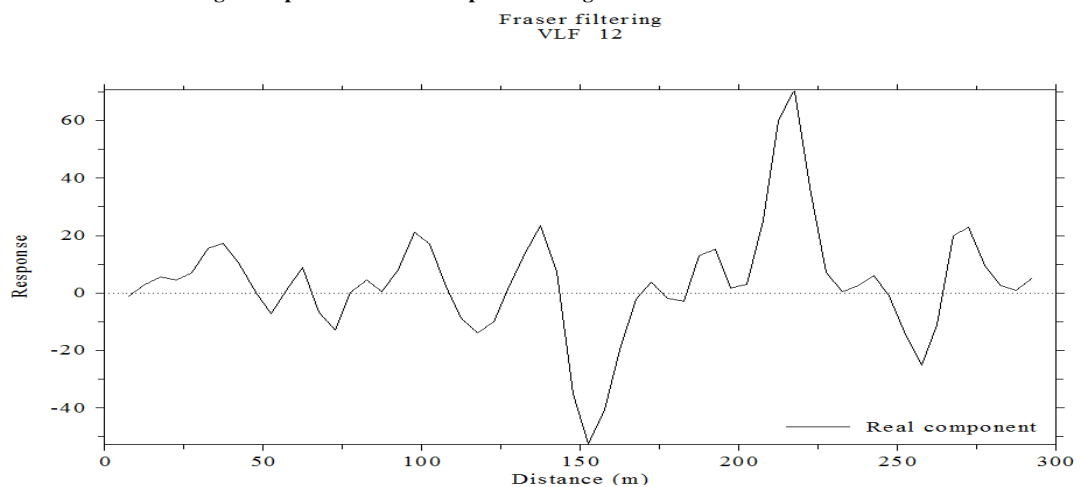


Fig 37: A plot of filtered in-phase data against distance at location VLF 12

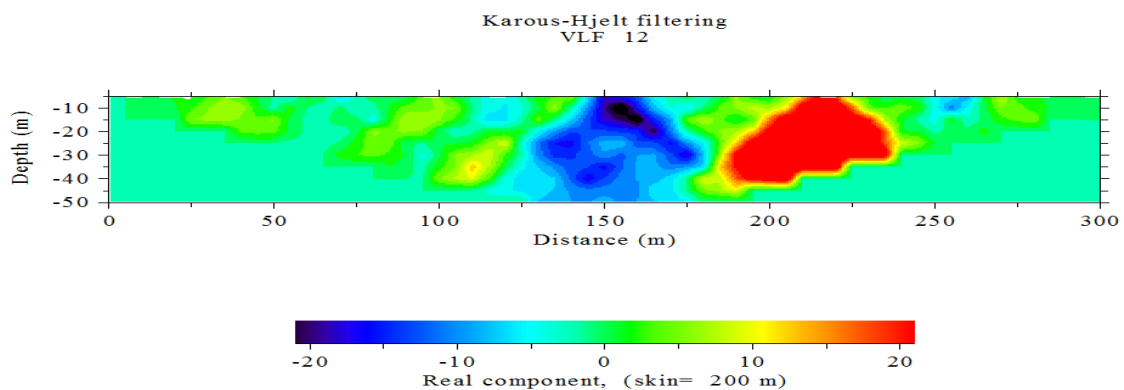


Fig 38: Current density cross section plot of in-phase data against distance at location VLF 12

CONCLUSION

The presence of and interconnectivity of fracture zones in the study area showed that the area has good prospects for groundwater development. It is therefore recommended that the search for groundwater in the study area should be aimed at searching for fracture zones where overburden is relatively thin and any borehole drilled in the study area should be made to pass through as many fracture zones as possible. This study recommends the drilling of productive and sustainable boreholes at locations VLF 01, VLF 03, VLF 06, VLF 08, VLF 10 and VLF 12 between 125-175m, 230-300m, 50-150m, 200-290m, 275-400m and 200-225m respectively along the profile.

Acknowledgements

The authors wish to acknowledge the cooperation of community Heads and the youths of the area in which this research was carried out.

REFERENCES

- [1] Haeni F P, Lane J W Jr, Lieblich DA, In: Banks, D. and Banks, S. (eds), memories of the XXIVth Congress, Oslo, Norway: *Inter. Assoc. of Hydrogeologist*, **1993**, 577-587.
- [2] Jansein J, Jurcek P, Voume II: Wheat Ridge, Colorado, *Env. and Engineering Geophysical Soc.*, **1997**, 635-644.
- [3] Lewis M R, Haeni F P, An annotated Bibliography: *US Geological Survey Circular*, **1987**.
- [4] Lieblich D A, Lane J W Jr, Haeni F P, (SEG), In Expanded Abstracts with Bibliographies SEG GIST Annual International Meeting vol. 1, **1991**.
- [5] Ekwueme B N, *Precambrian Res.*, **1990**, 47, 271-286
- [6] Ekwueme B N, *The Precambrian geology and evolution of the Southeastern Nigerian basement complex*. University of Calabar Press, **2003**, pp135
- [7] George A M, Okwueze E E, Akpan A E, Uchegbu C.J, *Nig. Journ. of Physics*, **2008**, 20(1), 136-144.
- [8] Iloeje, M. P., A new Geography of Nigeria, Longman, Nigeria, **1981**, p 26-28
- [9] Parasnis D S, *Mining Geophysics: Methods in Geochemistry and Geophysics*. Elsevier, Amsterdam, **1973**.
- [10] Sharma S P, Baranwal V C, *J of Appl. Geophy.*, **2005**, Vol. 37, 155-166.
- [11] McNeill J D, Labson V F, In Nabighian M C (Ed), *Soc. of Exploration Geophysicists*, **1991**, 191-218.
- [12] Alagbe O A, Sunmonu L A, Adabanija M A, *Res. Journ. of Physical Sciences*, **2013**, 1(3), 1-5.
- [13] Sunmonu L A, Alagbe O A, *Intern. Journ. of Phys.*, **2011**, 3(1), 70-75.
- [14] Rahman A A M S, Ukpogon E E, Azmatullah M, *J Min. Geol.*, **1981**, **18** (1), 60 – 65
- [15] Ekwere S J, Ekwueme B N, *Geologie en Mijnbouw*, **1991**, Vol. 70, 105-114.
- [16] Cross River State Government (CRSG), Report on preliminary investigation of economic mineral occurrences in Oban-Obudu basement complex, Cross River State, Nigeria, **1989**, 75.
- [17] Ekwere A S, Edet A, *Adv. in Applied Sci. Res*, **2012**, 3(1), 312-318
- [18] Ozezin K O, Oseghale A O, Ogedegbe E O, *Adv. in Applied Sci. Res*, **2012**, 3(1), 475-480
- [19] Deborah O O, Ayobami O A, *Adv. in Applied Sci. Res*, **2013**, 4(4), 420-431
- [20] Theophilus A A, Lukman A S, *Adv. in Applied Sci. Res*, **2012**, 3(5), 3142-3149
- [21] Jegede S I, Osazuwa I B, Ujuanbi O, Chiemeké C C, **2011**, 2(6), 1-8